Biophysical Journal, Volume 97

Supporting Material

Controlling the orientation and synaptic differentiation of myotubes with micropatterned substrates

Jacinthe Gingras, Robert M. Rioux, Damien Cuvelier, Nicholas A. Geisse, Jeff W. Lichtman, George M. Whitesides, L. Mahadevan, and Joshua R. Sanes

Controlling the orientation and synaptic differentiation of myotubes with micropatterned substrates

Jacinthe Gingras[1], Robert M. Rioux[2], Damien Cuvelier[3], Nicholas A. Geisse[4], Jeff W. Lichtman[1], George M. Whitesides[2], L Mahadevan[3], Joshua R. Sanes[1,*]

[1]Department of Molecular & Cellular Biology and Center for Brain Science, Harvard University, Cambridge, MA 02138
[2]Department of Chemistry & Chemical Biology, Harvard University, Cambridge, MA 02138
[3]School of Engineering and Applied Sciences, Department of Organismic & Evolutionary Biology, Harvard University, Cambridge, MA 02138
[4]Asylum Research, 6310 Hollister Avenue, Santa Barbara, CA 93117

Running title: Myotube alignment and differentiation

Key words: muscle, acetylcholine receptor, focal adhesion, tissue engineering, patterned surfaces

*Corresponding author:
sanesj@mcb.harvard.edu; (617) 496-8683 (p); (617) 496-0524 (f)

Supplemental Material

Table S1. Summary and sampled images of the different surface topography micropatterned into elastomeric poly(dimethylsiloxane) (PDMS) thin-films by soft lithography and their ability to induce alignment in myotube monolayers. The ability of the substrate to induce alignment in myotube monolayers and the measured angle is included for all of topographic elements in regular arrays -- square or hexagonal -- with constant separation between elements.

Figure S1. Influence of pattern height on the alignment of myotube monolayers on 20 μm × 20 μm square post arrays. (a) DIC images of a myoblast monolayer aligned over a large scale area (scale bar = 200 μm) . (b) Quantification of the number of branched myotubes on flast and three different 20 μm × 20 μm square post arrays heigths. (c) Patterned surfaces seemed to also influence the width of the myotubes such as 20 μm × 20 μm square post arrays of 3.5 μm heigth had the lowest standard deviation, hence the most regular width (24.3 μm).

Figure S2. DIC images of myotubes misaligned on 20 μm × 20 μm square post arrays of varying height, (a) 7.7 μm , (b) 9.9 μm and (c) 14.7 um. Scale bar = 40 μm

Figure S3. (a) DIC image of trypsinized myoblast. The spherical myoblast has a diameter of ~17.5 μm or a volume of ~2792 μm^3. (b) Fluorescence image of DAPI stained nucleus of myoblast from (a). (c) Overlay of DIC and fluorescence images. (d) Atomic force microscopy (AFM) image of a single myoblast straddling two diamonds (60 μm major-axis length). The image demonstrates that under conditions of low-confluency, the myoblast interacts strongly with adjacent diamonds. (e) A linescan over the area indicated in the inset of a myoblast straddling 60 μm major-axis length diamonds. The minimum height difference over the lammellapodium is 0.5 μm, while the maximum height along this scan is ~4 μm. Example of the different morphology of myoblasts observed in culture on topographically-patterned substrates include (f) 2-flap; (g) 3-flap; (h) 4-flap and (i) 4+-flap myoblast. (j) The dependence of myoblast morphology on confluency. The histogram demonstrates that at a cell density nearing confluency, myoblasts with a 2-flap morphology dominate the population. At lower confluence (25-30%), myoblasts tend to wet the surface and send out numerous processes (e.g. 4+-flap morphology), and only near full confluences are they in close enough proximity to each other that they adopt a 2-flap morphology. Scale bar = 10 μm.

Figure S4: Prediction and experimental data of myotubes growing on a diamond patterned surface (60 μm major-axis length, 3.5 μm tall). (a) Histogram representing the area covered by the ventral surface of the myoblast (footprint) relative to rotational angles along the features. A miximum footprint value is obtained at an angle of -3º , which is in agreement with the experimental data obtained. Examples of myotubes originating from (b) C2 cell lines and (c) primary myoblast grown and fused on such surfaces. (Scale bar = 20 μm)

Figure S5. Uniform laminin coating on patterned PDMS stamps (20 μm square posts separated by 20 μm, 3.5 μm tall) was confirmed by immunostaining the coated stamps (in the absence of cells) with an anti-laminin antibody and a fluorescent secondary antibody. As the number of rinses with PBS increased – (a) 3×, (b) 6× and (c) 9× – a more uniform coating of laminin is

observed compared to no rinses (panel d). We fixed the number of rinses at 9 to ensure a uniform coating over the entire surface of the stamps. Scale bar = 20 μm.

Square array of square posts		Alignment	Angle
20 μm side length 20 μm separation 3.5 μm tall	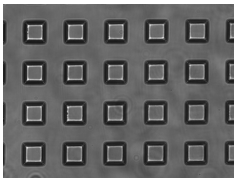	Yes (>7)	~25 degrees
20 μm side length 50 μm separation 3.5 μm tall	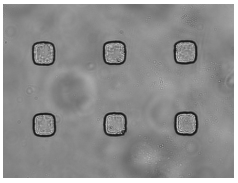	No (2)	random
20 μm side length 100 μm separation 3.5 μm tall	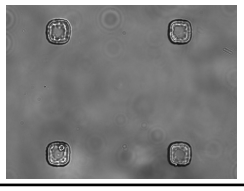	No (2)	random

Hexagonal array of square posts		Alignment	Angle
20 μm side length 20 μm separation 3.5 μm tall	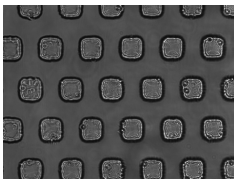	No (2)	random

Parallel line pattern		Alignment	Angle
20 μm width 20 μm separation 3.5 μm tall		Yes (>5)	~0 degree

Square array of circular posts		Alignment	Angle
20 μm diameter 20 μm separation 3.5 μm tall	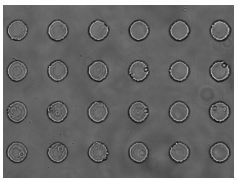	No (>4)	random

Hexagonal array of circular posts		Alignment	Angle
20 μm diameter 20 μm separation 3.5 μm tall	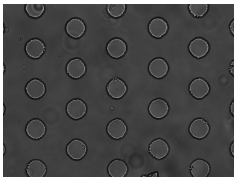	No (>2)	random

Hexagonal array of circular posts		Alignment	Angle
60 μm lengtth 20 μm separation 3.5 μm tall	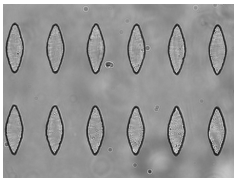	Yes (>5)	~5 degrees
40 μm length 20 μm separation 3.5 μm tall	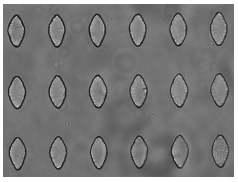	Yes (3)	~5 degrees

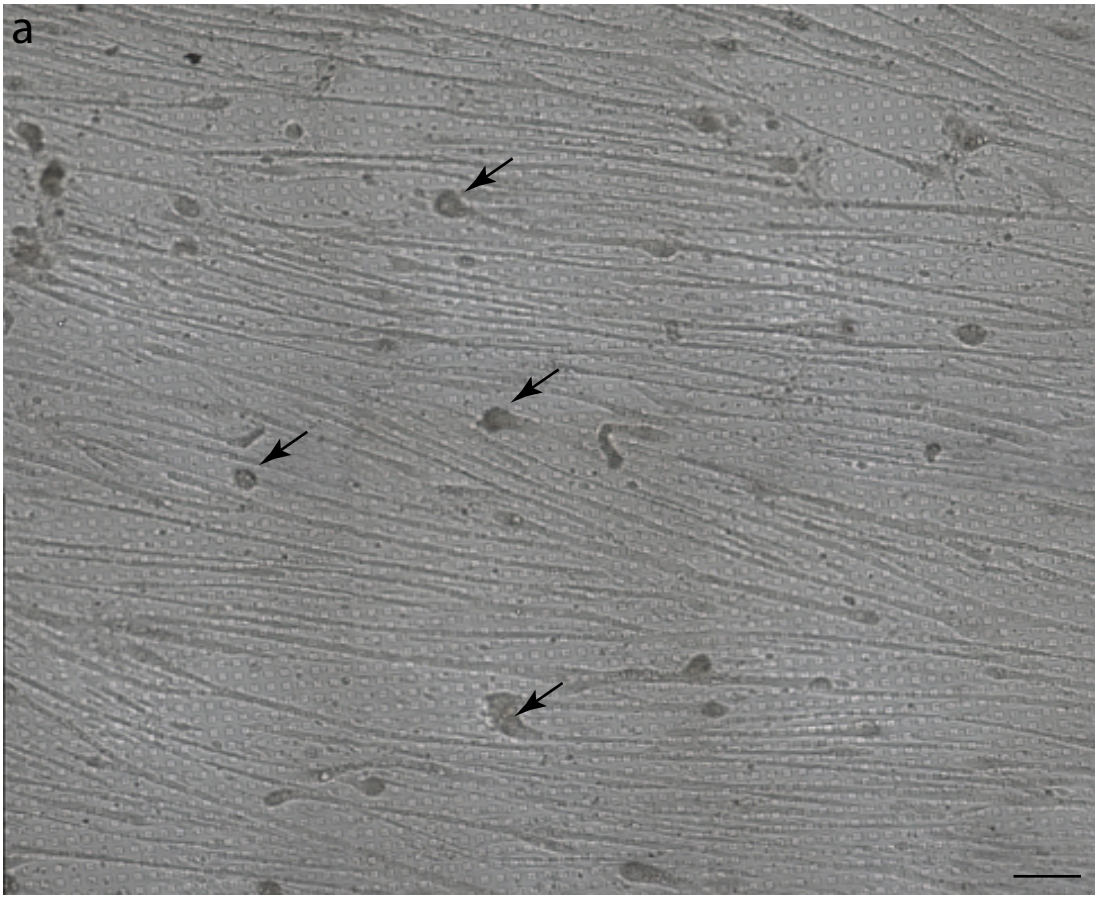

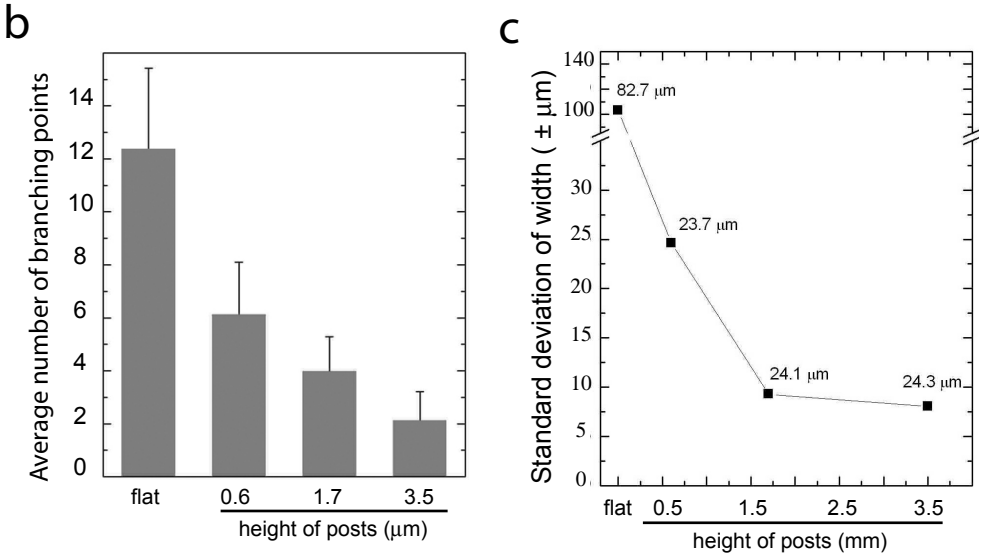

Supplemental Figure 1: Gingras et al.

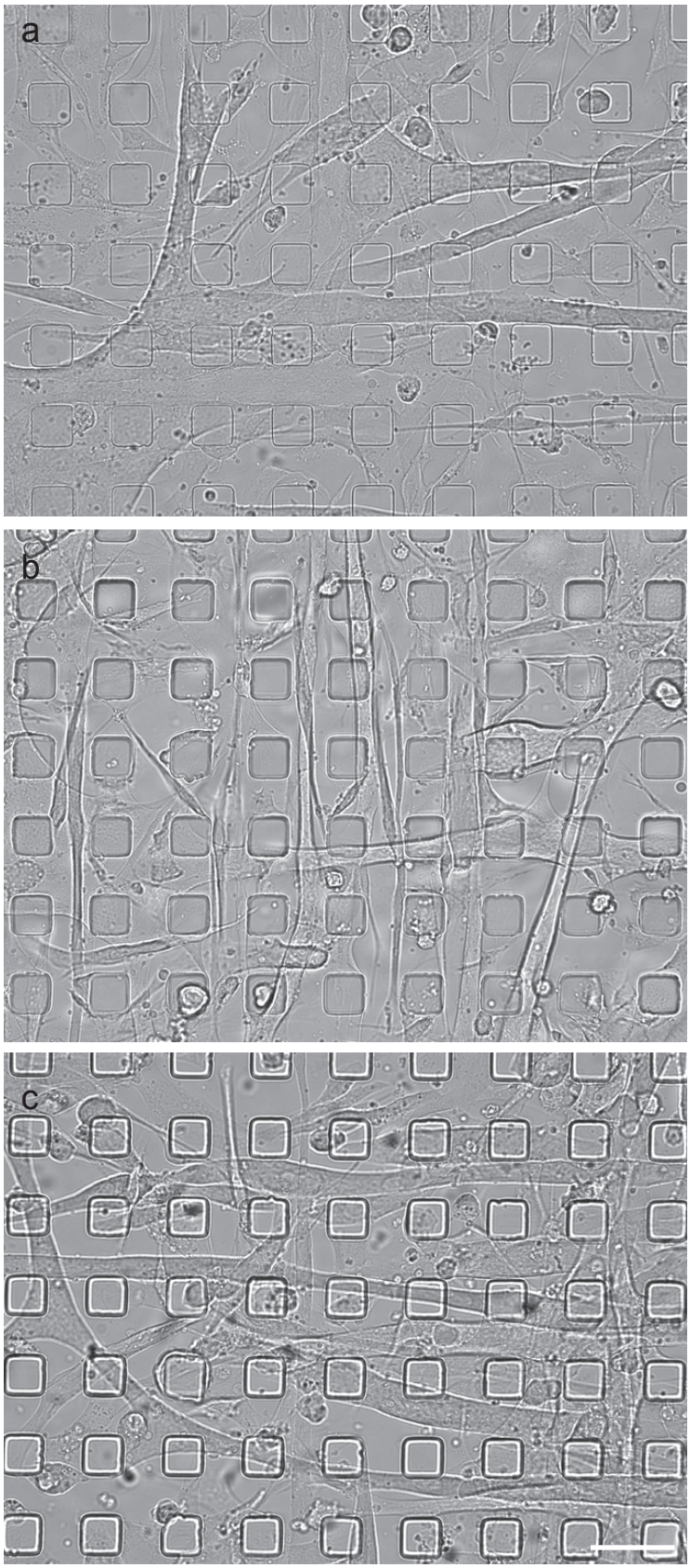

Supplemental Figure 2: Gingras et al.

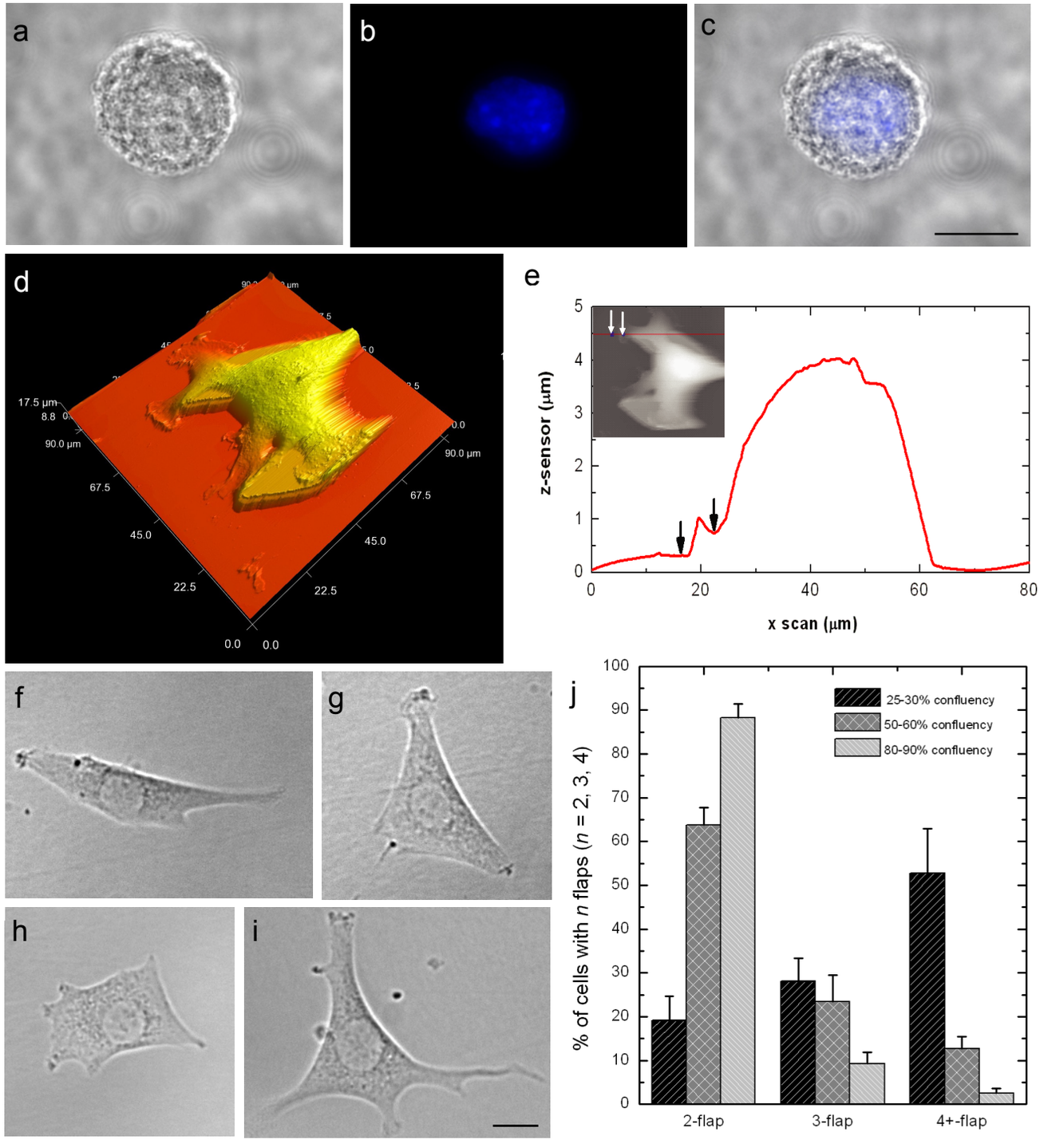

Supplemental Figure 3: Gingras et al.

a

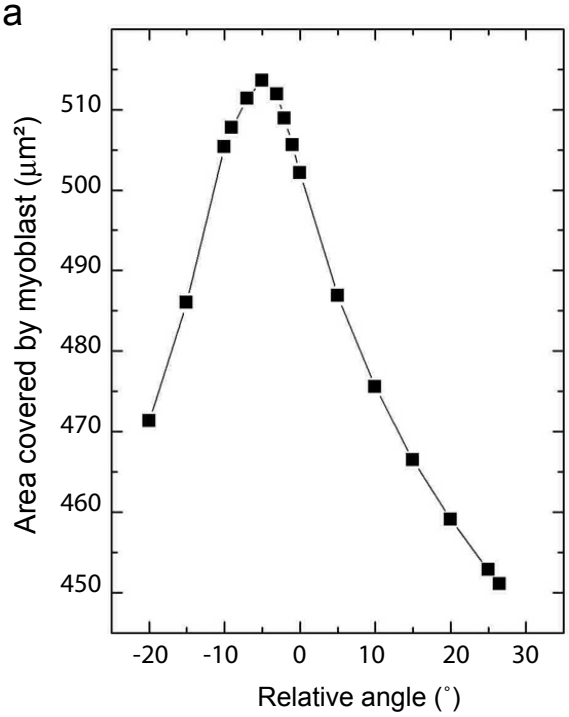

b

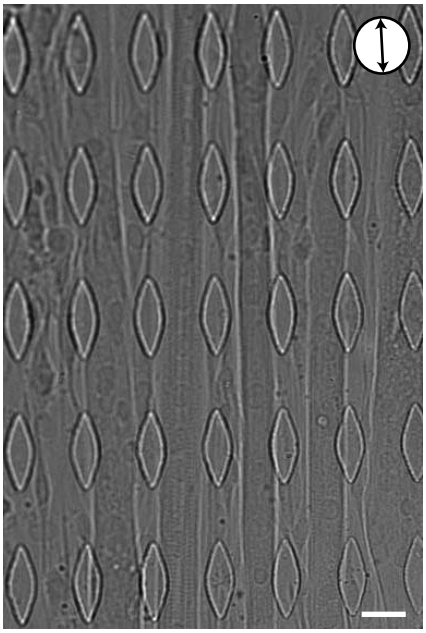

c

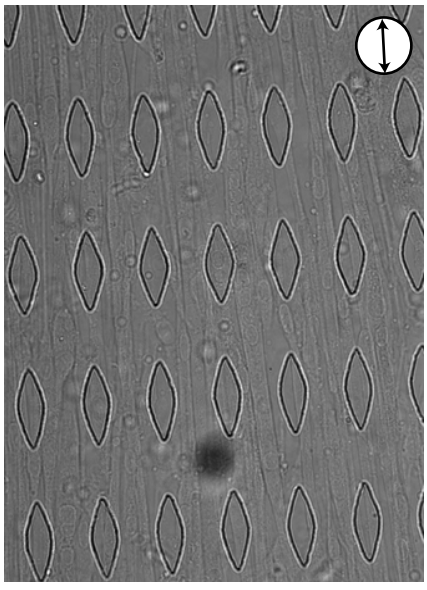

Supplemental figure 4: Gingras et al.

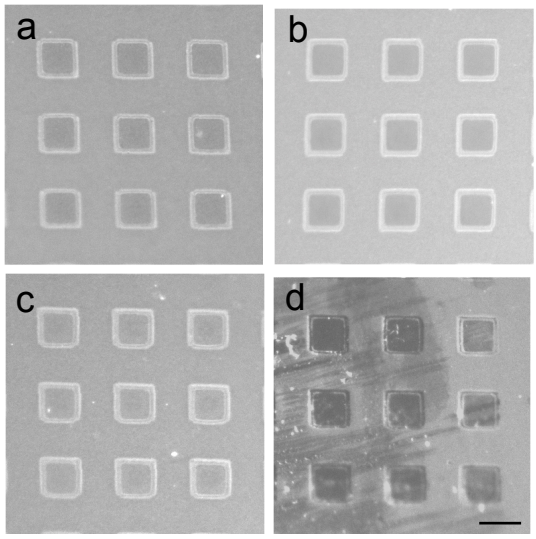

Supplemental figure 5: Gingras et al.